Chemical Geology 493 (2018) 246–257

Contents lists available at ScienceDirect

Chemical Geology

journal homepage: www.elsevier.com/locate/chemgeo

Quantification of paleo-aquifer changes using clumped isotopes in subaqueous carbonate speleothems

Fernando Gázquez[a,g,*], Andrea Columbu[b], Jo De Waele[b], Sebastian F.M. Breitenbach[c,a], Ci-Rong Huang[d], Chuan-Chou Shen[d], Yanbin Lu[e], José-María Calaforra[f], Maryline J. Mleneck-Vautravers[a], David A. Hodell[a]

[a] Department of Earth Sciences, University of Cambridge, Downing Street, Cambridge CB2 3EQ, United Kingdom.
[b] Italian Institute of Speleology, Department of Biological, Geological and Environmental Sciences, University of Bologna, Via Zamboni, 67, 40126 Bologna, Italy
[c] Sediment & Isotope Geology, Institute of Geology, Mineralogy & Geophysics, Ruhr-University Bochum, Universitätsstr, Bochum, Germany
[d] High-Precision Mass Spectrometry and Environmental Change Laboratory (HISPEC), Department of Geosciences, National Taiwan University, Taipei City 106, Taiwan, ROC
[e] Department of Earth Sciences, University of Minnesota, 310 Pillsbury Drive SE, Minneapolis, MN 55455-0231, USA
[f] Water Resources and Environmental Geology Research Group, University of Almería, Ctra. Sacramento s/n, 04120 Almeria, Spain
[g] School of Earth and Environmental Sciences, University of St. Andrews, St Andrews KY16 9AL, Scotland, United Kingdom

ARTICLE INFO

Keywords:
Calcite-aragonite
Clumped isotopes
Hydrothermal aquifer
Hypogene karst
Water temperature reconstruction
U/Th dating

ABSTRACT

Here we track the water-table position and temperature of the Mount San Giovanni aquifer (Iglesiente-Sulcis mining district, SW Sardinia, Italy) during the past 600 ka by determining the ages (U/Th dating) and stable isotope compositions ($\delta^{18}O$, $\delta^{13}C$ and Δ_{47}) of a variety of subaqueous carbonate speleothems (e.g. calcite spars, dogtooth calcite crystals and calcite coatings). Clumped isotopes (Δ_{47}) provide quantitative estimates of carbonate formation temperatures (and thus water temperatures) that are independent of the oxygen isotope composition of water ($\delta^{18}O_w$). Then, the $\delta^{18}O_w$ of the paleo-water has been reconstructed from the clumped isotope temperature ($T\Delta_{47}$) and the $\delta^{18}O$ of the carbonate ($\delta^{18}O_c$). We find that some high-temperature calcite spars formed prior to 600 ka at temperatures above ~120 °C. Lower-temperature spars (~70 °C) precipitated at ~400 ka, and cold-water subaqueous speleothems (~10–20 °C) formed in perched ponds at different levels of the karst systems between 410 ka and 110 ka, while coeval precipitation of subaerial flowstones occurred in the upper level of the shallower caves until 82 ka. We infer that the groundwater level dropped by ~120 m from ~400 to ~250 ka, with a relatively rapid rate of ~0.8 mm/yr. Considering the tectonic stability of Sardinia during the Quaternary, this high rate derives from climate driven geomorphological processes at the surface rather than tectonic uplift. The $\delta^{18}O$ values of the paleo-aquifer water range from -6.0 ± 0.7‰ during MIS 5c, and similar to modern cave water values (−5.1‰), to -7.7 ± 0.4‰ during the colder MIS 8. These values indicate that the groundwater reflected the $\delta^{18}O$ signal of meteoric water, with no significant contributions from metasomatic and metamorphic waters. The observed $\delta^{18}O_w$ variability can be explained by glacial/interglacial paleoclimate changes affecting rainfall $\delta^{18}O$ (and thus groundwater $\delta^{18}O$). We conclude that clumped isotope thermometry on subaqueous carbonate speleothems is a useful tool for tracking paleo-aquifer temperatures and $\delta^{18}O_w$ reconstructions.

1. Introduction

Hypogene speleogenesis caused by rising of CO_2/H_2S-rich fluids is, contrary to what was thought only a decade years ago, a common karstification process that generated dozens of caves worldwide (see Klimchouk et al., 2017, for a recent review on hypogenic caves). Signs of hydrothermal fluid-rock interaction in caves include geomorphological features (Audra et al., 2002, 2007, 2009; De Waele and Forti, 2006; Klimchouk, 2007, 2009; Stafford et al., 2008; Palmer, 2011; Calaforra and De Waele, 2011; Klimchouk et al., 2012; De Waele et al., 2013, 2016), evidence for bedrock alteration (Dublyansky and Spötl, 2009; Palmer and Palmer, 2012; Plan et al., 2012; Gázquez and Calaforra, 2013) and characteristic cave minerals and speleothems (Polyak and Provencio, 2001; Davis, 2000, Davis, 2012; Audra et al., 2009, 2015; Forti, 2010; Pagliara et al., 2010; Leél-Őssy et al., 2011; De Waele et al., 2013, 2016; Gázquez et al., 2013a, 2017), often with

* Corresponding author.
E-mail address: f.gazquez@ual.es (F. Gázquez).

https://doi.org/10.1016/j.chemgeo.2018.05.046
Received 6 April 2018; Received in revised form 26 May 2018; Accepted 31 May 2018
Available online 02 June 2018

distinctive geochemical compositions (LaRock and Cunningham, 1995; Dublyansky and Spötl, 2009; Palmer and Palmer, 2012; Decker et al., 2015).

Unlike epigenic caves, corrosion/precipitation of carbonates in hypogene systems is not controlled by CO_2 inputs from the soil and vegetation coverage or exchange with external atmospheric air, but has its origin in deeper processes (metasomatism and metamorphic mechanisms releasing CO_2; Klimchouk et al., 2017) or in the dissolution of the carbonate host rock as thermal fluids ascend. Carbonate corrosion/precipitation is given by the reaction:

$$CaCO_3\,(s) + CO_2\,(g) \uparrow + H_2O \leftrightarrow 2HCO_3^- + Ca^{?+}$$

Ca^{2+}–HCO_3^--rich waters can precipitate carbonate minerals (i.e. calcite or aragonite) when the equilibrium reaction is displaced to the left. This is generally accompanied by CO_2-degassing, evaporation and/or water temperature lowering (Audra et al., 2009). Such conditions are prone to occur when the fluids rise to the upper level of hydrothermal aquifers and the hydrostatic pressure decreases, as water approaches the top of the aquifer, moving away from the deeper thermal source. Indeed, the shallower sectors of many hypogene karst systems generally show greater abundance of secondary carbonate formations, compared to deeper areas that often display mainly dissolution features (Audra et al., 2009; Gázquez and Calaforra, 2013).

Carbonate speleothems can be deposited in subaqueous and subaerial conditions, if CO_2 degassing occurs below or above the water body surface respectively. Subaqueous speleothems can furthermore be subdivided into phreatic (usually formed tens of meters below the water table), epiphreatic (formed in shallow aquifer levels that can be emerget because of occasional water table lowering) (Jennings, 1985) and vadose (formed in pools/lakes in caves well above the water table). Note that in other studies, the term “phreatic” has been used to refer to overgrowth speleothems (POS) deposited close to the water table in anchialine caves (e.g. Fornós et al., 2002), which would be classified as *epi*phreatic speleothems following the classification used in the present study.

Typical subaqueous carbonate speleothems in hypogene caves include calcite spars and dogtooth crystals (LaRock and Cunningham, 1995; De Waele et al., 2013; Gázquez et al., 2013b; Decker et al., 2015; Vardanjani et al., 2017), and mammillary coatings (Polyak et al., 2013; De Waele et al., 2017; Gázquez et al., 2017), whereas folia (e.g. Audra et al., 2009; Leél-Őssy et al., 2011; Davis, 2012; Gázquez and Calaforra, 2013; Polyak et al., 2013), calcite rafts and calcite raft cones (e.g. Jones, 1989; Hill and Forti, 1997; Davis, 2000; Piccini, 2000; Audra et al., 2002; Leél-Őssy et al., 2011; Polyak et al., 2013; Gázquez and Calaforra, 2013; Piccini et al., 2015), are typical of shallower (epi) phreatic levels or the oscillation zone. The mechanisms involved in the formation of each type of speleothem are generally associated with specific environmental conditions. For example, calcite raft cones form exclusively in relatively shallow (less than few meters deep) subterranean water pools, and therefore, can be used as indicators of paleo-aquifer levels (Gázquez and Calaforra, 2013; De Waele et al., 2017; Kovacs et al., 2017). However, some types of subaqueous carbonate speleothems are not exclusive of hypogene caves but are also found in low-temperature epigenic caves (e.g. cave cones and folia; Wildberger, 1987; Plan and De, 2011; Davis, 2012; Fornós et al., 2002; D'Angeli et al., 2015a; De Waele et al., 2017; Kovacs et al., 2017).

Assuming that subaqueous carbonate speleothems precipitate in isotopic equilibrium with water and no significant kinetic effects occur during carbonate crystallization, the oxygen isotope composition of calcite can be used to reconstruct the water temperature at the time of mineral precipitation. This is because the oxygen isotope fractionation factor (α) between HCO_3^- (previously equilibrated with H_2O) and $CaCO_3$ is sensitive to temperature (Urey, 1948). This temperature relationship for calcite precipitation in cave environments was postulated by Coplen (2007) to be represented by the expression:

$$1000 \ln \alpha = 17.4\,(10^3\,T^{-1}) - 28.6 \quad (1)$$

where, α depends on the oxygen isotope compositions (standardized with respect to the international reference material Vienna Standard Mean Ocean Water, V-SMOW) of the carbonate ($\delta^{18}O_c$) and the water ($\delta^{18}O_w$) at the time of mineral precipitation, and T is the water temperature in K. $\delta^{18}O_c$ can be determined by isotope ratio mass spectrometry (Spötl and Vennemann, 2003), while $\delta^{18}O_w$ is generally obtained from the analysis of fluid inclusions trapped in calcite (Arienzo et al., 2013) or $\delta^{18}O_w$ in groundwaters of known age (Talma and Vogel, 1992).

An alternative to the $\delta^{18}O_c$-$\delta^{18}O_w$ approach is the determination of the actual formation temperature of carbonates via clumped isotope thermometry. This paleothermometer is based on the temperature dependence of the $^{13}C—^{18}O$ clumping into bonds within the carbonate mineral lattice, expressed as Δ_{47}(Ghosh et al., 2006; Eiler, 2007) and is independent of the $\delta^{18}O_w$ for temperature calculations. Instead, $\delta^{18}O_w$ can be back-calculated from $\delta^{18}O_c$ and the clumped temperature ($T\Delta_{47}$). Unfortunately, the application of clumped isotopes to subaerial speleothems (i.e. stalagmites) has been limited in many cases by the lack of understanding of equilibrium/disequilibrium processes during carbonate precipitation from thin water films in vadose cave environments (Affek et al., 2008; Daëron et al., 2011; Kluge et al., 2014a). However, recent clumped isotope analyses of mammillary coatings in Devil's Hole (Nevada, US) suggest that subaqueous carbonate formed under isotope equilibrium conditions between 180 ka and 27ka, and therefore, water temperatures could be calculated (Kluge et al., 2014b). Also, $T\Delta_{47}$ obtained from recent subaqueous cave pearls formed in different climatic settings, matches the water temperature of the pool waters from which it formed (Breitenbach et al., 2018). This suggests that, under certain conditions, subaqueous cave carbonates can precipitate in thermodynamic and isotopic equilibrium with water and clumped isotope thermometry can be used for paleo-temperature reconstructions. In addition to low-temperature carbonates, clumped isotope thermometry has been recently applied to infer the temperature of paleo-waters by using calcite spars (Budd et al., 2013) and hydrothermal dolomite (Ferry et al., 2011) formed in deep environments.

Here we combine clumped isotope thermometry and classic $\delta^{18}O$ and $\delta^{13}C$ measurements in calcite/aragonite to reconstruct paleo-water temperature and $\delta^{18}O_w$ in Mount San Giovanni (SW Sardinia, Italy) during the Late Quaternary (< 600 ka to 82 ka). The various crystalline habits and arrangement of speleothems in the caves of Mount San Giovanni suggest that carbonate formed under different environmental conditions, including change to various distances from the water surface (subaqueous/subaerial conditions), water geochemistry and temperatures. However, the exact environmental settings in which these speleothems crystallized have not been constrained yet. In addition to temperature, clumped isotopes on subaqueous speleothems have been used to calculate $\delta^{18}O_w$ values of the paleo-aquifer. The significance of the different types of speleothems and potential paleoclimatic implications are discussed, including variations in the water table, water geochemistry and temperature changes with time.

2. Geological setting

Mount San Giovanni Mine is located in the Iglesiente region (SW Sardinia, Italy), a Pb—Zn mining district active since pre-Roman times (Cidu et al., 2009) (Fig. 1). Most mines exploited Mississippi Valley Type ore bodies hosted in Lower Cambrian limestones and dolostones (Bechstadt and Boni, 1996). The carbonate succession starts with grey dolostones (Santa Barbara Fm.), followed by darker massive dolostones and a thick succession of whitish-grey intensely karstified limestones (San Giovanni Fm.).

The San Giovanni Mine exploited a very rich E-W oriented, 2 km long and 700 m wide ore body (Brusca and Dessau, 1968) hosted in the southern limb of the Iglesias syncline (Civita et al., 1983). This ore was

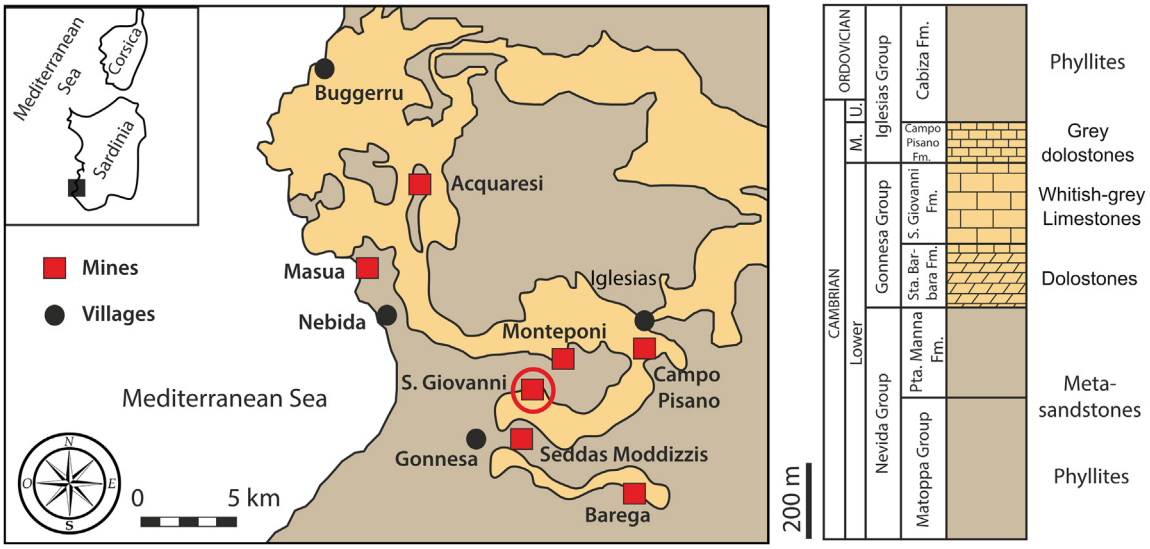

Fig. 1. Geological map of the Iglesiente-Sulcis mining district (SW Sardinia, Italy) and location of the Mount San Giovanni mine (after Caddeo et al., 2011).

excavated from the top of the mountain (400 m a.s.l.) to around 250 m below sea level, and around 100 km of mine galleries have been excavated through Mount San Giovanni. Ore exploitations lasted until 1998, when pumping operations in a nearby (connected) mine was discontinued in 1997 and the water table rapidly rose back to its original level at around 60 m a.s.l. (Cidu et al., 2011).

During tunnel construction many karst voids were intercepted. A total of over 50 caves have been mapped in this mine, most of which lack a natural entrance (so called "mine caves"; Messina et al., 2005; Pagliara et al., 2010; De Waele et al., 2013, 2017; Gázquez et al., 2013b). Despite the fact that some caves have been now for long time (the most interesting from a scientific point of view being Santa Barbara 1 cave, discovered in April 1952; Rossetti and Zucchini, 1956), multidisciplinary scientific researches began only recently (Pagliara et al., 2010; Caddeo et al., 2011; De Waele et al., 2013; Gázquez et al., 2013b).

Mine levels hosting significant numbers of caves are located between 170 and 226 m a.s.l. (Figs. 2 and 3). In the Peloggio tunnel (218 m a.s.l.) a sequence of small caves was intercepted, including Crovassa Azzurra cave (Caddeo et al., 2011). This cave is composed of two superposed chambers, connected by a shaft, and hosts a wide variety of speleothems and mineralizations, such as blue aragonite flowstones, and calcite dogtooth spars. The Idina gallery (150 m a.s.l.) intercepts a large mineralized karst void extending from this level up to the surface (370 m a.s.l.). Between 160 and 180 m a.s.l. a section of a speleothem-rich natural cave has been saved from mining activities and is known as Crovassa Ricchi in Argento cave. The richest mine tunnel is known as Albert (~226 m a.s.l.), which intercepted at least eight important caves. Massa Riccardo cave is located in its upper portion and descends into a large room, the floor of which is located at around 205 m a.s.l. (Figs. 2 and 3).

3. Materials and methods

3.1. Samples

In 2005 a core 8 cm in diameter and 0.5 m long (sample GA-core) was retrieved from an aragonite/calcite flowstone located at ~2 m below the cave entrance of Crovassa Azzurra (216 m a.s.l., Figs. 3 and 4E). The core was sampled using a hand-held water-cooled HILTI® drilling machine with a 30 cm long drill bit and extensions. The core was split lengthwise and 11 subsamples for U/Th dating were taken (Fig. 4D). In the 2012 sampling campaign, the void left by the 2005 core extraction was found filled with dripwater, and a sample of this water was collected for isotopic analysis.

In addition to the cores samples, carbonate samples from three caves of the Mount San Giovanni mine were collected in 2012 (Table 1, Fig. 3). Six samples were collected in Crovassa Azzurra cave. A fragment of calcite coatings detached from the cave ceiling was collected at ~5 m below the cave entrance (208 m a.s.l., Fig. 3). The inner part of this sample consists of a pristine scalenohedral calcite spar (~10 cm in size) that is coated with a layered calcite crust (~15 cm thick)

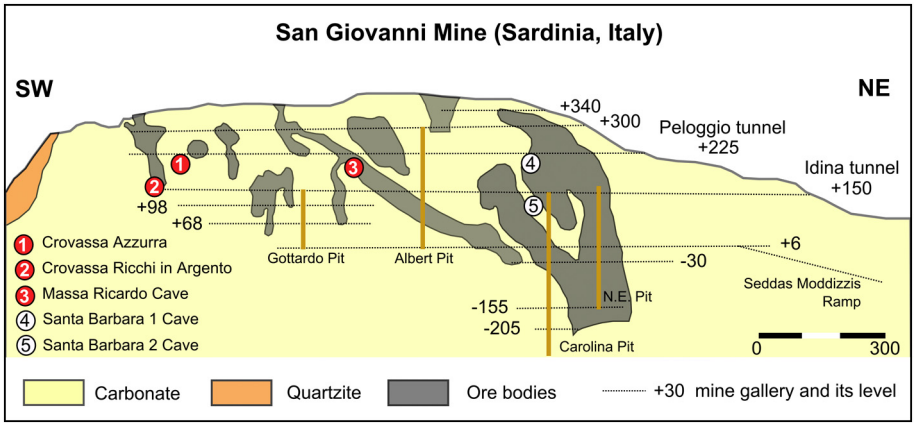

Fig. 2. Cross-section of the Mount S. Giovanni mine (after De Waele et al., 2013) with the locations of the studied caves, the main ore bodies and the mine galleries and shafts indicated in grey. Sampled caves in this study are shown in red. (For interpretation of the references to colour in this figure legend, the reader is referred to the web version of this article.)

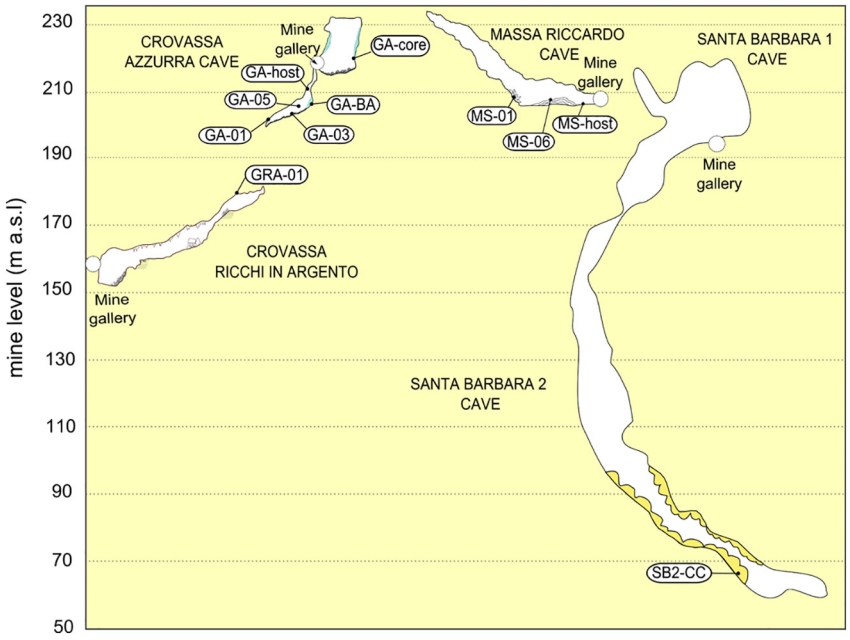

Fig. 3. Topographic profile of caves Crovassa Azzurra, Crovassa Ricchi in Argento, Massa Riccardo and Santa Barbara (after Messina et al., 2005), showing the sampling sites: GA-05 (calcite spar and calcite coatings); GA-01 (calcite dogtooth crystals); GA-core (flowstone core); GA-03 (calcite spars); GA-BA (blue aragonite flowstone); GRA-01 (calcite spars); MS-01 (calcite roses); MS-06 (calcite spar and flowstone); GA-host and MS-host (host rock); SB2-CC. Mammillary calcite coatings (cave clouds) analyzed by De Waele and Forti (2006). Note the relative positions of the caves in the X axis have been modified for graphical representation.

composed of whitish and brownish laminae (Fig. 4A). Two additional scalenohedral calcite spars (~15 cm in size each) were collected from the cave floor at 205 m a.s.l. Also, three dogtooth calcite speleothems were taken from the cave walls at ~12 m below the cave entrance (at 201 m a.s.l. in Fig. 3 and Fig. 4B). A fragment of blue aragonite flowstone was collected from the cave floor (208 m a.s.l.) as well as a sample of the carbonate host rock.

In Crovassa Ricchi in Argento cave, four scalenohedral calcite spars were collected in 2012 from the floor in different parts of the cave, at around 180 m a.s.l. (Figs. 3). In Massa Riccardo cave (Fig. 3), fragments of a whitish calcite flowstone (~20 cm thick) that deposited on a scalenohedral calcite spar (Fig. 4D), were collected at 206 m a.s.l. Two samples of euhedral calcite, composed of aggregates of ~3 cm in size planar calcite crystals resembling "roses" were collected from the cave wall (Fig. 4C) at 208 m a.s.l. A fragment of the carbonate host rock was taken from the wall of Massa Riccardo cave.

Homogeneous carbonate powders from the cleanest part of all the specimens described above were obtained using a Dremel® drill tool. In addition, we consider for interpretations the U/Th age of a mammillary calcite coating (cave clouds) taken in 2005 in Santa Barbara 2 cave at 65 m a.s.l. and reported by De Waele and Forti (2006) (SB2-CC in Fig. 3).

3.2. U/Th dating

Seven carbonate subsamples, 100–200 mg each, were selected from calcite spars, dogtooth calcite crystals, aragonite flowstones and calcite crusts, and eleven subsamples of drilled flowstone cores from Crovassa Azzurra cave were analyzed for U/Th dating at the *High-precision mass spectrometry and environment change* lab (HISPEC) at the National Taiwan University. We followed the chemical procedure described by Edwards et al. (1987) and Shen et al. (2012) to separate uranium and thorium. A gravimetrically calibrated (Cheng et al., 2013) triple-spike, ^{229}Th-^{233}U-^{236}U, isotope dilution method was employed to correct mass bias and determine U/Th contents and isotopic compositions (Cheng et al., 2000; Shen et al., 2012). U/Th isotopic compositions and ^{230}Th dates were determined by a multi-collector inductively coupled plasma mass spectrometer (MC-ICPMS), Thermo Fisher Neptune (Shen et al., 2012; Cheng et al., 2013). Half-lives of U/Th nuclides used for ^{230}Th age calculation are given in Cheng et al. (2013). Ages were corrected by assuming an initial ^{230}Th/^{232}Th atomic ratio of $4.4 \pm 2.2 \times 10^{-6}$ (see Table S1 for details). Uncertainties in the U/Th isotopic data and uncorrected-corrected ages are given at the two sigma (2σ) level or two standard deviations of the mean ($2\sigma_m$) unless otherwise stated (Table S1).

3.3. $\delta^{18}O$ and $\delta^{13}C$ in carbonates

Powdered carbonate samples ($n = 32$, ~200 μg each) were flushed with CP grade helium in Exetainer tubes (Labco®), then acidified with 104% H_3PO_4 and left to react for 1 h at 70 °C. Stable carbon and oxygen isotopes of CO_2 were measured using a ThermoScientific GasBench II, equipped with a CTC autosampler coupled to a MAT253 mass spectrometer (Spötl and Vennemann, 2003) in the Godwin Laboratory at the University of Cambridge, UK. Analytical precision was estimated at ± 0.03‰ for $\delta^{13}C$ and ± 0.08‰ for $\delta^{18}O$ by repeated analysis of an inhouse Carrara Marble standard. Results are reported in ‰ relative to the Vienna PeeDee Belemnite (V-PDB) reference.

3.4. Clumped isotopes

Seven samples of subaqueous carbonate speleothems (i.e. calcite spars, dogtooth calcite crystals and calcite coatings), were investigated for their clumped isotope composition (Δ_{47}, Table 1 and supplementary Table S2). Note that no samples from the GA-core were analyzed for Δ_{47}, because it is interpreted as having formed in subaerial conditions and may have been affected by isotopic disequilibrium during precipitation (Affek et al., 2008; Daëron et al., 2011; Kluge et al., 2014a). Powder aliquots of 120 to 140 μg each were loaded in borosilicate vials and analyzed on a KIEL-IV device, coupled to a ThermoFinnigan MAT253 mass spectrometer in the Godwin Laboratory at the University of Cambridge, UK (for details see Breitenbach et al., 2018). Between 16 and 37 aliquots per sample were analyzed over a period of several months. Acid digestion using 104% orthophosphoric acid was performed at 70 °C. The four carbonate standards ETH1, ETH2, ETH3 and ETH4 were used for normalization (Meckler et al., 2014) and errors are reported as 2-standard error of the mean of the aliquots measured. The relationship between Δ_{47} and temperature for low temperature carbonate speleothems (i.e. $\Delta_{47} > 0.5$‰) was determined using our in-house calibration, which is based on natural subaqueous cave carbonates formed at temperatures between 3 and 47 °C (Breitenbach et al., 2018, $\Delta_{47} = (0.0447 \pm 0.006)*10^6/T^2 + (0.149 \pm 0.07)$; where T in K and

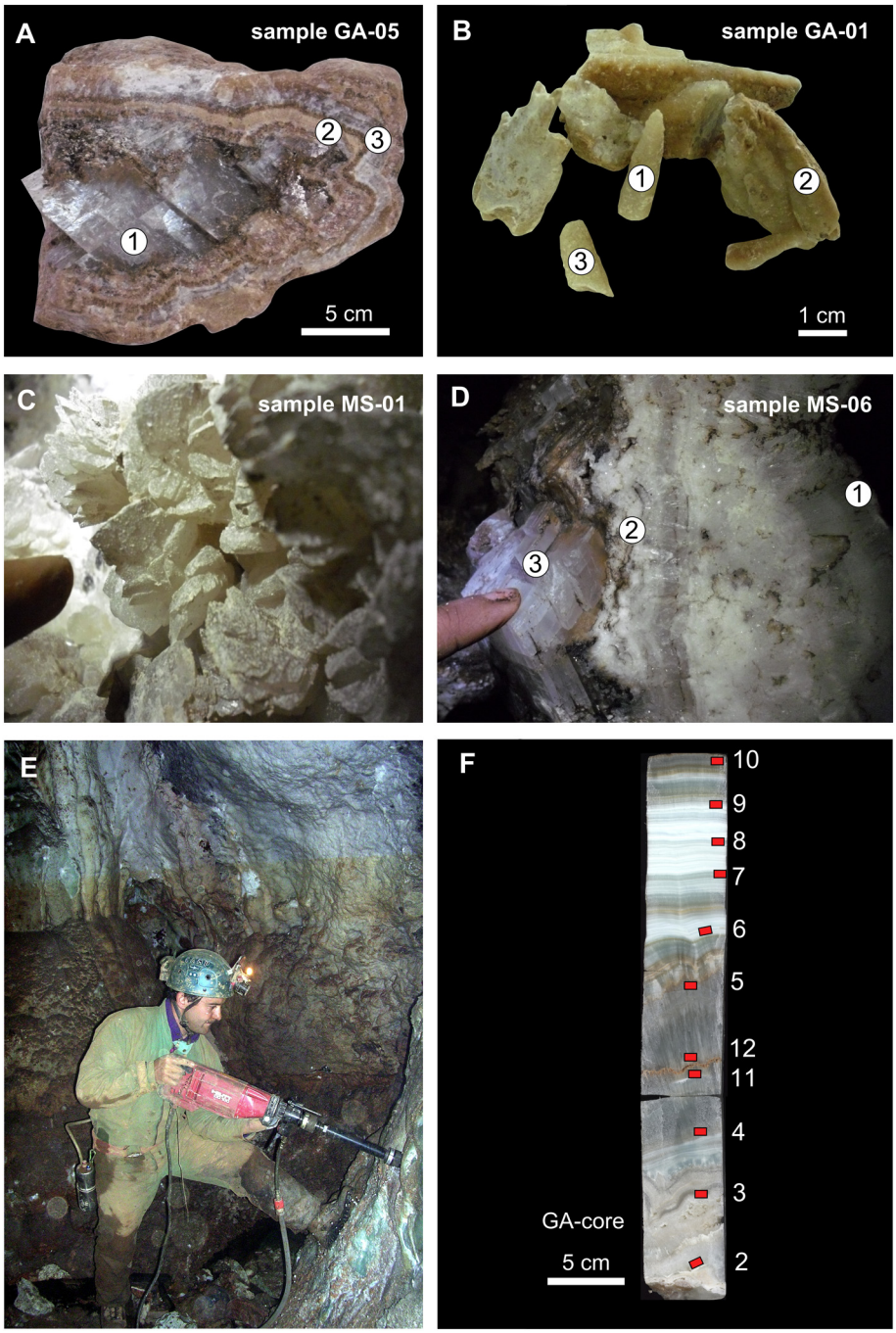

Fig. 4. Overview on the speleothem samples analyzed in this study; A. Scalenohedral calcite spar (subsample GA-05-1) covered with white and brownish calcite coatings (subsamples GA-05-3 and GA-05-2, respectively) collected in Crovassa Azzurra cave; B. Dogtooth calcite crystals from the lower levels of Crovassa Azzurra cave (subsamples GA-01-1, GA-01-2 and GA-01-3); C. Calcite "roses" from Massa Riccardo cave (subsamples MS-01-1 and MS-01-2); D. Scalenohedral calcite spar (subsample MS-06-3) covered with white calcite flowstone (subsamples MS-06-1 from the top and MS-06-2 from the base) collected in Massa Riccardo cave. E and F. Sampling of the flowstone core in Crovassa Azzurra cave (sample GA-core) and position of eleven subsamples for U/Th dating.

Δ_{47} in ‰; Eq. 2). For higher temperatures (i.e. Δ_{47} < 0.5‰), we used the Δ_{47}-temperature calibration of Kele et al. (2015) ($\Delta_{47} = (0.044 \pm 0.005)*10^6/T^2 + (0.205 \pm 0.0504)$; where T in K and Δ_{47} in ‰; Eq. 3). Both calibration equations were obtained using the same parameters and standards, but the Breitenbach et al. (2018) calibration is used here for low-temperature samples, because it is based on the same type of subaqueous cave carbonates.

4. Results

4.1. U/Th dating

^{238}U content in the dated samples varies between aragonite and calcite, although in both polymorphs concentrations are relatively high (Table S1). In aragonite, ^{238}U is always higher than 1000 ppb, while in calcite the average is 476 ppb (min: 8 ppb, max: 1642 ppb). The content of non-authigenic ^{232}Th is higher for calcite and lower for aragonite (Table S1); however, the $^{230}Th/^{232}Th$ activity ratio (which together with the error associated with the calculation of $^{238}U/^{234}U/^{230}Th/^{232}Th$ rules the uncertainties associated with the final ages) is generally high (> 50). Consequently, all ages reported have relatively low 2σ-errors (except sample GA-CORE-2, which is close to the U/Th dating limit).

U/Th results indicate that speleothems in the Mount San Giovanni karst system formed between > 600 ka and 82.3 ± 0.3 ka BP (Table 1). The " > 600 ka" notation refers to samples out of the range of the dating method, which is currently between 600 and 800 ka BP depending on the U/Th characteristics of the sample under analysis (Hellstrom, 2003; Cheng et al., 2013). The flowstone core sampled in Crovassa Azzurra (GA-core) started to grow beyond this limit, with basal ages of 684 ± 244 and > 500 ka BP (GA-core-2 and 3, Table 1).

Table 1
Sample locations and descriptions, isotopic analyses, U/Th ages (± 2SD) (see supplementary Table S1 for details) and temperature estimates using clumped isotopes thermometry (TΔ_{47} ± 2SE). The number of aliquots analyzed (n) is given. The actual $\delta^{18}O_w$ (± 2SE) of the paleo-aquifer has been calculated from the TΔ_{47} and $\delta^{18}O_c$ using eq. 1 in the main text (see supplementary Table S2 for calculations and propagation of analytical uncertainties). Water temperatures are also calculated using the $\delta^{18}O_c$-$\delta^{18}O_w$ approach ($T^{18}O_c$-$^{18}O_w$), assuming that the paleo-$\delta^{18}O_w$ was −5.5 ± 1‰ (2SE) for all samples, a value similar to the modern cave water (see discussion for details), using eq. 1 for calcite samples and the paleotemperature equation of Kim et al. (2007) for aragonite samples. The $\delta^{18}O_c$-$\delta^{18}O_w$ approach gives temperature uncertainties of ± 5 °C (2SE). *sample analyzed by De Waele and Forti (2006).

Sample	Depth (m a.s.l)	Description	Formation environment	$\delta^{18}O_c$ (‰ VPDB)	$\delta^{13}C$ (‰ VPDB)	Age (ka)	T($^{18}O_c$-$^{18}O_w$) (°C)	Δ_{47} (‰)	T Δ_{47} (°C)	$\delta^{18}O_w$ (‰ VSMOW)
CROVASSA AZZURRA										
GA-05-1	208	Scalenohedral calcite spar	Subaqueous (high temperature)	−13.6	−0.5	394 ± 13	69	–	–	–
GA-05-2	208	Calcite crust (brown layer)	Subaqueous (low temperature)	−4.6	−9.7	–	17	–	–	–
GA-05-3	208	Calcite crust (white layer)	Subaqueous (low temperature)	−4.6	−7.9	410 ± 14	17	0.696 ± 0.012 (*n* = 19)	13 ± 3	−6.4 ± 0.7
GA-01-1	201	Dogtooth calcite crystals	Subaqueous (low temperature)	−5.1	−8.1	109 ± 0.5	20	0.680 ± 0.013 (n = 16)	17 ± 3	−6.0 ± 0.7
GA-01-2	201	Dogtooth calcite crystals	Subaqueous (low temperature)	−4.3	−6.3	216 ± 1.3	16	0.694 ± 0.013 (*n* = 20)	14 ± 3	−6.0 ± 0.7
GA-01-3	201	Dogtooth calcite crystals	Subaqueous (low temperature)	−4.2	−6.2	–	16	–	–	–
GA-BA-1	208	Aragonite flowstone (white layer)	Subaerial (low temperature)	−4.3	−5.7	–	12	–	–	–
GA-BA-2	208	Aragonite flowstone (blue layer)	Subaerial (low temperature)	−4.1	−4.3	383 ± 10	11	–	–	–
GA-03-1	205	Scalenohedral calcite spar	Subaqueous (high temperature)	−18.8	−0.3	–	109	0.476 ± 0.018 (n = 20)	130 ± 14	−3.1 ± 1.5
GA-03-2	205	Scalenohedral calcite spar	Subaqueous (high temperature)	−15.6	0.1	–	83	–	–	–
GA-core-2	216	Flowstone core (36 cm from the top)	Subaerial (low temperature)	−5.1	−8.9	684 ± 244	16	–	–	–
GA-core-3	216	Flowstone core (31.5 cm from the top)	Subaerial (low temperature)	−4.8	−11.1	> 600	14	–	–	–
GA-core-4	216	Flowstone core (27 cm from the top)	Subaerial (low temperature)	−4.3	−9.1	570 ± 53	12	–	–	–
GA-core-11	216	Flowstone core (22.5 cm from the top)	Subaerial (low temperature)	−4.5	−8.2	587 ± 44	14	–	–	–
GA-core-12	216	Flowstone core (21.5 cm from the top)	Subaerial (low temperature)	−4.6	−6.2	581 ± 51	15	–	–	–
GA-core-5	216	Flowstone core (16.6 cm from the top)	Subaerial (low temperature)	−4.1	−8.4	506 ± 19	11	–	–	–
GA-core-6	216	Flowstone core (12 cm from the top)-aragonite	Subaerial (low temperature)	−4.8	−7.6	228 ± 2	14	–	–	–
GA-core-7	216	Flowstone core (8.5 cm from the top)-aragonite	Subaerial (low temperature)	−4.4	−7.4	208 ± 1	12	–	–	–
GA-core-8	216	Flowstone core (6 cm from the top)-aragonite	Subaerial (low temperature)	−5.2	−7.2	198 ± 1	16	–	–	–
GA-core-9	216	Flowstone core (3.6 cm from the top)-aragonite	Subaerial (low temperature)	−4.9	−6.8	193.6 ± 0.8	14	–	–	–
GA-core-10	216	Flowstone core (0.5 cm from the top)	Subaerial (low temperature)	−4.5	−6.5	82.3 ± 0.3	13	–	–	–
GA-host	210	Host rock	–	−10.4	−0.8	–	–	–	–	–
MASSA RICCARDO										
MS-06-1	206	Calcite flowstone (top)	Subaerial (low temperature)	−4.4	−10.1	–	16	–	–	–
MS-06-2	206	Calcite flowstone (bottom)	Subaerial (low temperature)	−5.1	−10.2	–	20	–	–	–
MS-06-3	206	Scalenohedral calcite spar	Subaqueous (medium temperature)	−7.0	−8.4	–	29	–	–	–
MS-01-1	208	Calcite “roses”	Subaqueous (low temperature)	−4.4	−10.4	–	16	–	–	–
MS-01-2	208	Calcite “roses”	Subaqueous (low temperature)	−5.2	−10.4	265 ± 6	23	0.708 ± 0.008 (*n* = 37)	10 ± 2	−7.7 ± 0.4
MS-host	207	Host rock	–	−11.7	−0.2	–	–	–	–	–
CROVASSA RICCHI IN ARGENTO										
GRA-01-1	180	Scalenohedral calcite spar	Subaqueous (high temperature)	−18.8	−0.3	> 600	109	0.485 ± 0.009 (n = 20)	123 ± 6	−3.8 ± 0.6
GRA-01-2	180	Scalenohedral calcite spar	Subaqueous (high temperature)	−18.2	0.2	–	105	–	–	–
GRA-01-3	180	Scalenohedral calcite spar	Subaqueous (high temperature)	−18.8	0.1	–	109	0.491 ± 0.012 (*n* = 18)	119 ± 9	−4.3 ± 1.0
GRA-01-4	180	Scalenohedral calcite spar	Subaqueous (high temperature)	−18.6	0.2	–	109	–	–	–
SANTA BARBARA 2 CAVE										
SB2-CC*	65	Mammillary calcite coatings	Subaqueous (medium temperature?)	–	–	247 ± 17	–	–	–	–

Its middle section, mostly characterized by cm-long fiber calcite, grew from 570 ± 53 to 506 ± 19 ka BP (GA-core 4 and 5), although an obvious hiatus occurs between 587 ± 44 and 581 ± 51 ka BP (GA-core 11 and 12), indicated by the presence of muddy brownish sediments. A similar hiatus appears above samples GA-core 5, and the next stratigraphically younger age is 228 ± 2 ka BP (GA-core 6). From here, a peculiar blue aragonitic flowstone was deposited without apparent major growth interruptions until 82.3 ± 0.3 ka BP (see Table 1 for intermediate ages). In the same cave, a similar blue aragonitic flowstone yielded an age of 383 ± 0.5 ka BP (GA-BA-2). This indicates that environmental conditions for the formation of subaerial blue aragonite flowstone were suitable at least since this time. Scalenohedral calcite spar and the overlying calcite crusts, formed slightly earlier, between 394 ± 13 and 410 ± 14 ka BP (GA-05-1 and 2). Conversely, dogtooth calcite crystals, sampled in the lower part of Crovassa Azzurra cave, were forming contemporaneously with the blue aragonite flowstone, considering their ages of 216 ± 1.3 and 109 ± 0.5 ka BP (GA-01-1 and 2). In Massa Riccardo cave, calcite roses were deposited since at least 264 ± 0.6 ka BP (sample MS-01-2). The scalenohedral calcite spar from Crovassa Ricchi in Argento returned out-of-range ages (> 600 ka BP, GRA-01-1). Finally, the mammillary calcite from Santa Barbara 2 cave (SB2-CC) is 247 ± 17 kyr old, as reported by De Waele and Forti (2006).

4.2. $\delta^{18}O$ and $\delta^{13}C$ analyses of carbonates and clumped isotopes (Δ_{47}) thermometry

Carbonate oxygen and carbon isotope values show two distinct groups of samples (Fig. 5). A first cluster is characterized by relatively low $\delta^{18}O_c$ values (−18.8‰ to −13.6‰), i.e. distinctly lower than the Cambrian carbonate host rock (−11.7‰ to −10.4‰), and relatively high and homogeneous $\delta^{13}C$ values (−0.3‰ to +0.2‰), similar to the host rock (−0.8‰ to −0.2‰). This cluster comprises all calcite spars, except one (MS-06-03) from Massa Riccardo cave that shows considerably higher $\delta^{18}O$ (−7.0‰) and lower $\delta^{13}C$ (−8.4‰) values.

The second cluster comprises the remaining samples, which show rather homogeneous $\delta^{18}O$ values, ranging −5.2‰ to −4.1‰, but a wider range of $\delta^{13}C$, from −11.1‰ to −4.3‰. In general, aragonite flowstone shows more positive $\delta^{13}C$ values (> −10‰), while most samples (i.e. calcite flowstones and calcite "roses") are grouped around −10.5‰. The dogtooth calcite crystals from Crovassa Azzurra cave show intermediate $\delta^{13}C$ values (−8.5‰ to −6.2‰).

The seven samples analyzed for clumped isotopes show Δ_{47} values ranging from 0.476‰ to 0.708‰ (Table 1 and supplementary Table S2). The uncertainties of the clumped isotope analyses are between 0.004‰ and 0.009‰ (1SE) or 0.008 to 0.018‰ as margin of error at the 95% confidence level. All the clumped isotope uncertainties and propagated errors for $T\Delta_{47}$ and $\delta^{18}O_w$ are given as 2-standard errors of the mean (2SE). The spar samples GA-03-1, GRA-01-1 and GRA-01-3 showed the lowest Δ_{47} value (0.476 ± 0.018‰, 0.485 ± 0.009‰ and 0.491 ± 0.012‰, respectively), whereas the calcite crust GA-05-03 (0.696 ± 0.012) and the dogtooth crystals (GA-01-01 and GA-01-02; 0.680 ± 0.013‰ and 0.694 ± 0.013‰, respectively) of Crovassa Azzurra cave and the calcite "roses" MS-01 of Massa Riccardo cave (0.708 ± 0.008‰) display higher Δ_{47}. After calibration using eq. 2 for Δ_{47} values > 0.5 and eq. 3 for Δ_{47} values < 0.5, the higher formation temperature corresponds to the calcite spars GA-03-01 (130 ± 14 °C), GRA-01-1 (123 ± 6 °C) and GRA-01-3 (119 ± 9 °C), whereas the rest of the samples formed at lower temperatures, ranging from 10 ± 2 °C to 17 ± 3 °C (Table 1).

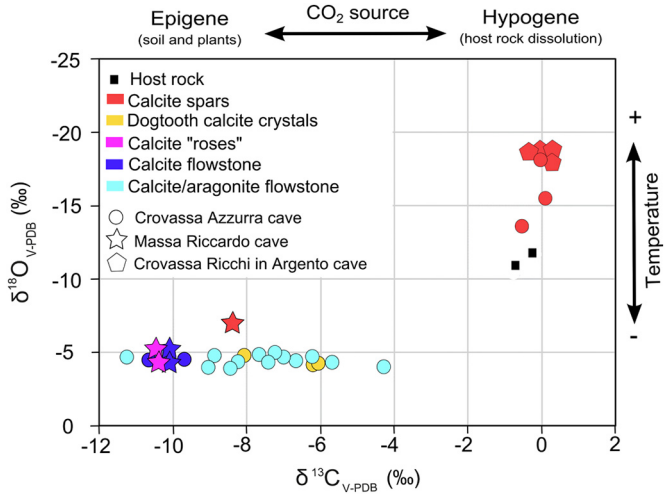

Fig. 5. Oxygen and carbon isotopes in carbonate samples from the caves of the Mount San Giovanni mine.

5. Discussion

5.1. Clumped isotope thermometry and paleo-aquifer $\delta^{18}O_w$ reconstruction

The clumped isotope results suggest that the paleo-aquifer of Mount St. Giovanni experienced pronounced cooling from the earlier (> 600 ka) stages, when calcite spar precipitated under deep-phreatic conditions, to the later (< 410 ka) phases of epiphreatic and subaerial speleothem formation. According to the Δ_{47} data from calcite spars (samples GA-03-1, GRA-01-1 and GRA-01-3, Table 1), the water temperature in the caves of the Mount San Giovanni was very high (probably > 120 °C) before > 600 ka, but decreased until 410 ± 14 ka and ranged from 10 ± 2 °C to 17 ± 3 °C until at least ca. 109 ± 0.5 ka. Given the limited number of samples analyzed and the analytical uncertainty of the measurements, small $T\Delta_{47}$ variations (e.g. 13 ± 3 °C to 17 ± 3 °C) are not interpreted here. Monitoring in Santa Barbara 1 cave carried out between 2001 and 2003 has shown cave temperature to range between 15 and 16 °C, and these temperatures are comparable to those measured from time to time in the other caves located roughly at the same altitude (Chiesi, 2005). This suggests that water temperature at the ~210 m level has been relatively cold (i.e. 10 to 20 °C) from at least 410 ± 14 ka until present.

Combining $T\Delta_{47}$ and $\delta^{18}O_c$ from the same speleothem, the $\delta^{18}O_w$ of the paleo-water can be calculated. The $\delta^{18}O_w$ value of the speleothem-forming water at ~410 ka was −6.4 ± 0.7‰ (sample GA-05-3) during the warmer-than-present marine isotope stage 11 (MIS 11). During the similarly warmer MIS 7 (~216 ka) and MIS 5c (~109 ka) the $\delta^{18}O_w$ were − 6.0 ± 0.7‰ and − 6.0 ± 0.7‰, respectively. These values roughly agree with the modern water $\delta^{18}O_w$ in the cave (−5.1‰) and the annual weighted mean $\delta^{18}O_w$ of rainfall in Sardinia (−4.8 ± 1.8‰, $n = 16$, at the IAEA stations at Cagliari and Capo Caccia, between 2001 and 2002). Previous investigations of the microthermometry of fluid inclusions coupled with $\delta^{18}O_c$ measurements on epiphreatic calcite speleothems (i.e. carbonates formed in pools) of unknown ages in caves of Masua mine (~15 km North from Mount San Giovanni), produced also low temperatures (15–20 °C) and $\delta^{18}O_w$ values of −4 to −5‰ (De Vivo et al., 1987), in good agreement with our observations. Interestingly, the $\delta^{18}O_w$ of the speleothem-forming water at ~264 ka, during the colder MIS 8 (−7.7 ± 0.4‰,) was ~2‰ lower than the modern $\delta^{18}O_w$ in the cave. These results suggest that the $\delta^{18}O_w$ of the cave water (and thus that of the rainfall over Sardinia) may have varied at least ~2‰ during the past 400 ka, including warmer (MIS 11, MIS 7 and MIS 5c) and colder (MIS 8) periods. Such differences might be explained by the temperature effect on the $\delta^{18}O$ of rainfall that tends to be lower during colder periods (Clark and Fritz, 1997), or other paleoclimatically driven processes affecting rainfall on glacial/interglacial timescale (Fairchild et al., 2006).

The undated – although likely > 600 ka, according to other U/Th dated spars – high-temperature calcite spar from Crovassa Azzurra and

Crovassa Ricchi in Argento caves (GA-03-1, GRA-01-1 and GRA-01-3) show $\delta^{18}O_w$ values between −3.1 ± 1.5‰ and − 4.3 ± 1.0‰. These values are slightly higher than the modern $\delta^{18}O$ observations of the rainfall and cave water and also higher than the reconstructed < 600 ka-old paleo-water $\delta^{18}O$. This may have been related to seawater ingression in the aquifer and seawater/freshwater mixing during the early stages of hydrothermal calcite precipitation (probably during the Neogene/early Quaternary). Alternatively, paleo-aquifer evaporation because of the "boiling" that enriched the water in ^{18}O or some contributions of water from deep geological processes (e.g. metasomatism and metamorphic water) that may have influenced the isotopic composition of the paleo-aquifer (Clark and Fritz, 1997).

It can be assumed that the $\delta^{18}O_w$ of the recharge to the aquifer is equal to the mean $\delta^{18}O_w$ of the rainfall in this region and varied between −5‰ and − 6.5‰ during the past 600 kyrs. Using mean $\delta^{18}O_w$ of −5.5 ± 1‰, we apply the $\delta^{18}O_c$-$\delta^{18}O_w$ approach (using eq. 1) to estimate the formation temperatures of all our carbonate speleothems, including those that were not analyzed for clumped isotopes (using eq. 1 for calcite samples, and the temperature equation for inorganic aragonite by Kim et al., 2007). Most speleothems formed at temperatures between 11 °C and 20 °C, except for calcite spars which return precipitation temperatures ranging from 33 °C to 110 °C (T, $^{18}O_c$-$^{18}O_w$ in Table 1). The discrepancies between the Δ_{47}-temperatures and the $^{18}O_c$-$^{18}O_w$-approach temperatures (up to ~20 °C in the case of some high-temperature spars) are assumed to be caused by temporal variations in $\delta^{18}O_w$ of the paleo-water, as discussed above.

5.2. Paleohydrological changes at Mount San Giovanni

Clumped isotope thermometry provides quantitative estimates of paleo-water temperatures from subaqueous carbonate speleothems. Along with U/Th ages, and stratigraphic/speleological observations (e.g. speleothem characterization), we reconstruct the evolution of the Mount San Giovanni paleo-aquifer during the Late Quaternary. In this karst system, subaqueous speleothem precipitation occurred in three different environments: i) phreatic settings, i.e. tens to hundreds of meters below the water table; ii) epiphreatic environments, i.e. less than tens of meters below the water table and; iii) long-standing or ephemeral cave pools, located above the local water table. However, much earlier, and before the groundwater reached calcium carbonate saturation and speleothems precipitated, karstification (corrosion/dissolution of the carbonate host rock) was the prevailing mechanism.

The earliest stages of speleogenesis (formation of karstic voids) date back to the Cambrian-Ordovician (De Waele et al., 2013), when the upwelling of thermal water and oxidation of sulfide ore bodies during repeated cycles of marine to continental environmental changes (Bechstadt and Boni, 1996) led to karstification via sulfuric acid speleogenesis (Fig. 6A). Active oxidation of polymetallic sulfide ore bodies occurred because of enhanced circulation of meteoric water inside the system (Fig. 6B); this oxygen-rich water forced intense alteration of sulfides and partial re-mobilization of ore mineralizations (De Vivo et al., 1987; Cortecci et al., 1989). Typical hypogene morphologies related to rising thermal fluids, including bubble trails, cupolas and megascallops (De Waele et al., 2013), probably developed during the more recent karstification interval since the Oligo-Miocene, up to present.

From the Oligocene to the Pliocene subaerial and subaqueous conditions alternated in the entire Iglesiente region, with periods of seawater ingression into the karst (De Vivo et al., 1987). Subsequent stages were marked by water temperature lowering, as the solution reached supersaturation in quartz (SiO_2) and calcite. First, quartz precipitated from highly saline solutions (13.3–23.3% NaCl eq.) at high temperature (70–112 °C) (De Vivo et al., 1987). Subsequently, the water temperature decreased and rhombohedral and scalenohedral spars of calcite (sometimes tens of centimetres in size) precipitated in voids of the bedrock from low-saline solutions, as suggested by less saline fluid inclusions in calcite spar crystals in Masua Mine (0.5–2.7% NaCl eq.) (De Vivo et al., 1987). Our U/Th data indicate that the earlier stages of hydrothermal calcite precipitation occurred before 600 ka BP, when the temperature of the aquifer was probably greater than 120 °C. The high-temperature calcite spar GRA-01-1 from Crovassa Ricchi in Argento cave is older than 600 ka BP and most likely contemporaneous to GRA-01-2, GRA-01-3 and GRA-01-4 (Table 1), as well as the spars GA-03-1 and GA-03-2 found in Crovassa Azzurra cave. Most high-temperature spars are relatively depleted in ^{18}O, with $\delta^{18}O_c$ values ranging from −18.8‰ to −13.6‰, typical of high temperature carbonates (e.g. LaRock and Cunningham, 1995; Dublyansky and Spötl, 2009; Palmer and Palmer, 2012; Decker et al., 2015), whereas their $\delta^{13}C$ values are within a narrow range from −0.5‰ to +0.2‰. These carbon isotope values are similar to the Cambrian carbonate host rock (−0.8‰ to −0.2‰) and suggest that the main source of dissolved inorganic carbon during this early stage was marine bedrock, with insignificant contributions from other sources (e.g. CO_2 from the overlying soil and vegetation) (Fig. 5).

Although the exact age of the early phases of calcite spar precipitation has not been determined, thermal conditions might have occurred much earlier than 600 ka BP (Fig. 6C). In fact, a phreatic stage of barite precipitation at around 50 °C has been suggested for the nearby Corona 'e Sa Craba Cave, ca. 10 km south of Mt. San Giovanni and at around 270 m a.s.l. The age of this episode remains unknown, although it has been estimated to have occurred during the Lower Miocene (ca. 20 Ma), when volcanic activity characterized this part of Sardinia (Sauro et al., 2014).

Thermal activity persisted until at least ~400 ka BP (Fig. 6D), as suggested from relatively low $\delta^{18}O_c$ at ~208 m a.s.l. in Crovassa Azzurra cave (~70 °C at 394 ± 13 ka BP; GA-05-1). However, even before that time (i.e. 684 ± 244 and 570 ± 53 ka BP) subaerial carbonate flowstones (the base of the GA-core) formed at low temperature (~12–16 °C) in the upper chamber of this cave, at 216 m a.s.l., where no sign of hydrothermal calcite precipitation has been found from ca. 600 ka to 83 ka BP. This testifies that, at ~500–400 ka, carbonate deposition in two sectors of the same cave occurred in radically different hydrogeochemical environments (Fig. 6D). This can be explained by the upper cave levels were affected by meteoric cold-water infiltration and were relatively isolated from the lower levels by > 10 m of carbonate rock.

The age of the cold-water calcite coatings (~13 ± 3 °C at 410 ± 14 ka; sample GA-05-3) deposited over the GA-05-1 spar, and thus stratigraphically younger than the euhedral calcite crystals, overlaps with the final stage of high-temperature hydrothermal activity recorded by this spar. Apparently, a shift from hydrothermal to low-temperature conditions occurred in the caves at ~400 ka at the ~208 m level. A plausible explanation for this sudden change is a rapid drop of the local water table and replacement of thermal water at the ~208 m level (e.g. the bottoms of Crovassa Azzurra, Massa Riccardo and Santa Barbara 1 caves) by cold water that occupied perched ponds fed by meteoric seepage (Fig. 6E). The local groundwater level may be tens of meters below the perched ponds, and although the aquifer water temperature may still be warm, this did not significantly affect the temperature of the perched waters that likely adjusted to the average external environmental temperature during some phases of MIS 11. The coexistence of a thermal aquifer and colder perched pools at higher levels in the same karst system and disconnected from the main groundwater level, has been reported from hydrothermal systems elsewhere (Gázquez et al., 2012a, 2012b, 2013a). The relatively low $\delta^{13}C$ values found in samples younger than 400 ka (−11.1‰ to −4.3‰), compared to the older calcite spars support the greater contribution of edaphic CO_2, and minor input of CO_2 of deep/hypogene origin, including Cambrian dolostone dissolution. The $\delta^{13}C$ values in low-temperature carbonate are consistent with CO_2 (and derived HCO_3^-) from plants (e.g. Bar-Matthews et al., 2010) and carbonate precipitation in perched pools disconnected from a main hydrothermal

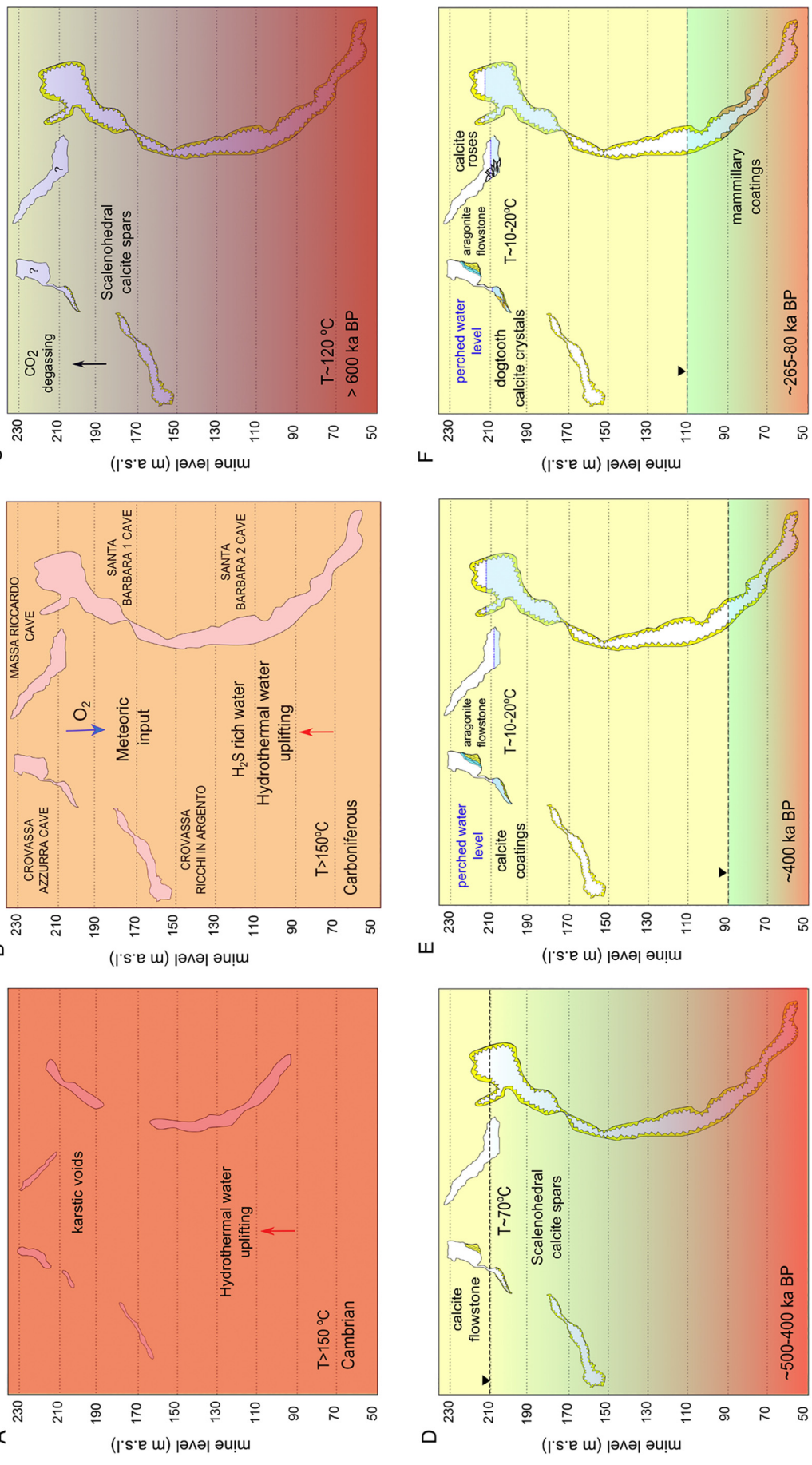

Fig. 6. Genetic evolution of the Mount San Giovanni caves. Estimated water table levels and temperatures are given in connection with precipitation of different types of speleothems: A. First stages of hypogene speleogenesis at high temperature during Cambrian; B. Intense karstification during the Carboniferous, probably related to H_2SO_4 produced due to oxidation of polymetallic sulfide ore bodies after increased O_2-rich meteoric water input; C. The first stages of hydrothermal calcite precipitation took place before 600 ka BP at temperature ~120 °C; D. Precipitation of hydrothermal (~70 °C) calcite spars and subaerial speleothem in the upper level of the karst coexisted between ~500 and ~400 ka BP; E. At ~400 ka BP, the water temperature decreased (~14 °C) and subaqueous calcite coatings formed in a perched pound covering hydrothermal spars formed during previous stages in Crovassa Azzurra cave. At the same time, subaerial aragonite flowstones formed in the upper level of this cave; F. Different types of epiphreatic speleothems (calcite dogtooth crystals and calcite roses) precipitated at low temperature (~10 °C to 20 °C) in perched pounds between 265 and 109 ka BP at the ~208 m level, while mammillary calcite coatings formed in deeper levels (~65 m a.s.l.) from the still warm, aquifer water. Meanwhile, aragonite flowstone kept growing until 82 ka BP. Note that the depth scale is illustrative and may have varied with time because of the exhumation of the karts.

reservoir.

After ~400 ka, no evidence is found that the local aquifer re-occupied the ~208 m level. Interestingly, mammillary calcite coatings (cave clouds) deposited under ephiphreatic conditions in the lower level of Santa Barbara 2 cave at 247 ± 17 ka (sample SB2-CC; De Waele and Forti, 2006), probably in a relatively warm aquifer. Cave clouds generally form in epiphreatic, warm environments, by a slow mechanism of CO_2 degassing close to the water table (some tens of meters below). Thus, at ~247 ka BP the water table probably was around 90 m a.s.l., at the same time that the calcite "roses" formed in a cold water perched pound in Massa Riccardo cave at 208 m a.s.l.

Our data suggest that the phreatic level may have dropped from 208 m a.s.l. at ~400 ka BP, to around 90 m a.s.l. at 247 ± 17 ka BP. The latter altitude is a conservative estimate, considering that the dated cave cloud in Santa Barbara 2 was not the highest one in this location (mammillary calcite cave clouds occur up to 10 m higher) (De Waele and Forti, 2006), and these peculiar speleothems can also form very close to the water surface (Hill and Polyak, 2010). Thus, the groundwater level dropped at least 120 m in 147 ± 30 kyrs, which is a rate of 0.82 $^{+0.2}/_{-0.14}$ mm/yr. Similar values are found in rapidly uplifting areas (Picotti and Pazzaglia, 2008; Columbu et al., 2015), but Sardinia is thought to be a relatively stable terrain at least for the last million years. A minimal (< 0.1 mm/year) uplift rate locally affected Sardinia (D'Angeli et al., 2015b) during the Late Quaternary, constituting ~14 ± 3 m absolute groundwater falling over this 147 ± 30 ka timeframe. Nevertheless, future detailed studies will investigate other processes triggering the remaining ~100 m drop. At this point of the research, we exclude higher uplift rates affecting the SW area of Sardinia and we point toward a prolonged downwearing of the phyllites (Fig. 1) surrounding the karst terrains at the surface. This low permeability rock, subjected to higher surface dismantling with respect to carbonates, constitutes an optimal impermeable boundary of the karst reservoir. Climate-driven processes (i.e. glacioeustatic sea-level variations, rainfall perturbations, etc.) might have intensified their weathering and incision, accelerating the drainage of the aquifer and thus the groundwater drop.

6. Conclusions

Clumped isotope thermometry, along with U/Th series dating of different types of carbonate speleothems from caves of the Mount San Giovanni mine have been used to reconstruct the temperature, isotope composition ($\delta^{18}O_w$) and the position of the groundwater level during the Late Quaternary. Subaqueous calcite spars were already forming before 600 ka at temperatures above ~120 °C, from a solution with $\delta^{18}O_w$ values slightly higher than the modern infiltration water in this region and the paleo-water $\delta^{18}O_w$ during the Late Quaternary reconstructed here.

Lower-temperature spars (~70 °C) and subaqueous flowstones continued precipitating at 393 ± 14 ka (MIS 11) at 208 m a.s.l., indicative of a cooling aquifer, while subaerial flowstones were forming at ~500 ka in upper level of the cave. Subsequent, stratigraphically younger, cold-water subaqueous carbonate coatings covering these spars formed in perched cave pools at approximately the same time (410 ± 14 ka), within analytical errors. At 265 ± 6 ka, the aquifer temperature remained cold, whereas subaqueous dogtooth calcite crystals formed between 216 ± 1 ka and 109 ± 0.5 ka in a subterranean pool at lower temperatures. Subaerial flowstones continued forming above 210 m a.s.l., for at least 300 ka (from 383 to 82 ka), stopping their growth only when climate became dry during MIS 5b.

Our data suggest that the water level fell by ~120 m from ~400 to ~250 ka; which is a rapid rate of ~0.8 $^{+0.2}/_{-0.14}$ mm/yr, never observed for the tectonically stable Sardinian landmass. Therefore, we suggest that such a high rate has been the result of climate-driven surface weathering of less permeable bounding geological formations (i.e. phyllites) that, prior to ~400 ka, confined the karst reservoir.

The reconstructed $\delta^{18}O_w$ values of the paleo-aquifer during MIS 11, MIS 8, MIS 7 and MIS 5c differ by < 2‰ from the modern cave water and meteoric water in the region. This $\delta^{18}O_w$ results can be of interest for future quantitative paleo-temperature reconstructions from subaerial speleothems in Sardinia and the Mediterranean region. We conclude that subaqueous speleothems, formed in either phreatic or epiphreatic environments are a powerful tool for reconstructions of environmental changes in paleo-aquifers, with potential implications for paleoclimate and paleohydrology research.

Supplementary data to this article can be found online at https://doi.org/10.1016/j.chemgeo.2018.05.046.

Acknowledgements

We thank James Rolfe and Ian Mather for technical assistance in the Godwin Laboratory. This study was supported by the NERC project, ID NE/M003752/1 to D.A.H. The sampling surveys were supported by the Water Resources and Environmental Geology Research Group (University of Almería). S.F.M.B., F.G. and D.A.H. acknowledge support from the European Union's Horizon 2020 Research and Innovation programme for project "QUEST" (Marie Sklodowska-Curie grant agreement No. 691037). U/Th dating was supported by the Science Vanguard Research Program of the Ministry of Science and Technology (MOST) (106-2628-M-002-013 to C-C.S.), the National Taiwan University (105R7625 to C-C.S.), and the Higher Education Sprout Project of the Ministry of Education, Taiwan ROC (107L901001 to C-C.S.). The authors are grateful to Professor Philippe Audra and two anonymous reviews, who contributed to improve the original manuscript.

References

Affek, H.P., Bar-Matthews, M., Ayalon, A., Matthews, A., Eiler, J.M., 2008. Glacial/interglacial temperature variations in Soreq cave speleothems as recorded by 'clumped isotope' thermometry. Geochim. Cosmochim. Acta 72, 5351–5360.

Arienzo, M.M., Swart, P.K., Vonhof, H.B., 2013. Measurement of ^{18}O and ^{2}H values of fluid inclusion water in speleothems using cavity ring down spectroscopy compared with isotope ratio mass spectrometry. Rapid Commun. Mass Spectrom. 27, 2616–2624.

Audra, P., Bigot, J.Y., Mocochain, L., 2002. Hypogenic caves in Provence (France). Specific features and sediments. Acta Carsol. 31 (3), 33–50.

Audra, P., Hobléa, F., Bigot, J.Y., Nobécourt, J.C., 2007. The role of condensation in thermal speleogenesis: study of a hypogenic sulfidic cave in Aix-les-Bains, France. Acta Carsol. 36 (2), 185–194.

Audra, P., Mocochain, L., Bigot, J.Y., Nobécourt, J.C., 2009. The association between bubble trails and folia: a morphological and sedimentary indicator of hypogenic speleogenesis by degassing, example from Adaouste cave (Provence, France). Int. J. Speleol. 38 (2), 93–102.

Audra, P., Gázquez, F., Rull, F., Bigot, J.Y., Camus, H., 2015. Hypogene sulfuric acid Speleogenesis and rare sulfate minerals in Baume Galinière cave (Alpes-de-Haute-Provence, France). Record of uplift, correlative cover retreat and valley dissection. Geomorphology 247, 25–34.

Bar-Matthews, M., Marean, C.W., Jacobs, Z., Karkanas, P., Fisher, E.C., Herries, A.I.R., Brown, K., Williams, H.M., Bernatchez, J., Ayalon, A., Nilssen, P.J., 2010. A high resolution and continuous isotopic speleothem record of paleoclimate and paleoenvironment from 90 to 53 ka from pinnacle point on the south coast of South Africa. Quat. Sci. Rev. 29, 2131–2145.

Bechstadt, T., Boni, M. (Eds.), 1996. Sedimentological, Stratigraphical and Ore Deposits Field Guide of the Autochtonous Cambro-Ordovician of Southwestern Sardinia. Memorie Descrittive Della Carta Geologica d'Italia 48. Servizio Geologico Italiano, Roma, pp. 390.

Breitenbach, S.F.M., Mleneck-Vautravers, M.J., Grauel, A.-L., Lo, L., Bernasconi, S.M., Müller, I.A., Rolfe, J., Gázquez, F., Greaves, M., Hodell, D.A., 2018. Coupled Mg/Ca and clumped isotope analyses of foraminifera provide consistent water temperatures. Geochim. Cosmochim. Acta. http://dx.doi.org/10.1016/j.gca.2018.03.010. (In press).

Brusca, C., Dessau, G., 1968. I giacimenti piombo-zinciferi di S. Giovanni (Iglesias) nel quadro della geologia del Cambrico sardo. L'Industria Mineraria 19, 1–53.

Budd, D.A., Frost III, E.L., Huntington, K.W., Allwardt, P.F., 2013. Syndepositional deformation features in high-relief carbonate platforms: long-lived conduits for diagenetic fluids. J. Sediment. Res. 82, 12–36.

Caddeo, G.A., De Waele, J., Frau, F., Railsback, L.B., 2011. Trace element and stable isotope data from a flowstone in a natural cave of the mining district of SW Sardinia (Italy): evidence for Zn^{2+}-induced aragonite precipitation in comparatively wet climatic conditions. Int. J. Speleol. 40 (2), 181–190.

Calaforra, J.M., De Waele, J., 2011. New peculiar cave ceiling forms from Carlsbad

caverns (New Mexico, USA): the zenithal ceiling tube-holes. Geomorphology 134, 43–48.
Cheng, H., Edwards, R.L., Hoff, J., Gallup, C.D., Richards, D.A., Asmerom, Y., 2000. The half-lives of U-234 and Th-230. Chem. Geol. 169, 17–33.
Cheng, H., Edwards, R.L., Shen, C.-C., Polyak, V.J., Asmerom, Y., Woodhead, J., Hellstrom, J., Wang, Y., Kong, X., Spötl, C., Wang, X., Alexander, E.C., 2013. Improvements in ^{230}Th dating, ^{230}Th and ^{234}U half-life values, and U-Th isotopic measurements by multi-collector inductively coupled plasma mass spectrometry. Earth Planet. Sci. Lett. 371-372, 82–91.
Chiesi, M., 2005. Il pre-monitoraggio dei parametri ambientali della Grotta di Santa Barbara (Miniera di San Giovanni, Iglesias). (premonitoring of the environmental parameters in the Santa Barbara Cave). Memorie dell'Istituto Italiano di Speleologia 2 (17), 23–34.
Cidu, R., Biddau, R., Fanfani, L., 2009. Impact of past mining activity on the quality of groundwater in SW Sardinia (Italy). J. Geochem. Explor. 100 (2), 125–132.
Cidu, R., Frau, F., Da Pelo, S., 2011. Drainage at abandoned mine sites: natural attenuation of contaminants in different seasons. Mine Water Environ. 30 (2), 113–126.
Civita, M., Cocozza, T., Forti, P., Perna, G., Turi, B., 1983. Idrogeologia del bacino minerario dell'Iglesiente (Sardegna sud-occidentale). Memorie dell'Istituto Italiano di Speleologia 2 (2), 1–139.
Clark, I.D., Fritz, P., 1997. Environmental Isotopes in Hydrogeology. Lewis Publishers, USA.
Columbu, A., De Waele, J., Forti, P., Montagna, P., Picotti, V., Pons-Branchu, E., Hellstrom, J., Bajo, P., Drysdale, R., 2015. Gypsum caves as indicators of climate-driven river incision and aggradation in a rapidly uplifting region. Geology 43, 539–542.
Coplen, T.B., 2007. Calibration of the calcite–water oxygen-isotope geothermometer at Devils Hole, Nevada, a natural laboratory. Geochim. Cosmochim. Acta 71, 3948–3957.
Cortecci, G., Fontes, J.C., Maiorani, A., Perna, G., Pintus, E., Turi, B., 1989. Oxygen, sulfur, and strontium isotope and fluid inclusion studies of barite deposits from the Iglesiente-Sulcis mining district, southwestern Sardinia, Italy. Mineral. Deposita 24 (1), 34–42.
Daëron, M., Guo, W., Eiler, J., Genty, D., Blamart, D., Boch, R., Drysdale, R.N., Maire, R., Wainer, K., Zanchetta, G., 2011. ^{13}C-^{18}O clumping in speleothems: observations from natural caves and precipitation experiments. Geochim. Cosmochim. Acta 75, 3303–3317.
D'Angeli, I.M., De Waele, J., Ceballo Melendres, O., Tisato, N., Sauro, F., Grau-Gonzalez, E., Bernasconi, S.M., Torriani, S., Bontognali, T.R.R., 2015a. Genesis of folia in a non-thermal epigenic cave (Matanzas, Cuba). Geomorphology 228, 526–535.
D'Angeli, I.M., Sanna, L., Calzoni, C., De Waele, J., 2015b. Uplifted flank margin caves in telogenetic limestones in the Gulf of Orosei (central-East Sardinia—Italy) and their palaeogeographic significance. Geomorphology 231, 202–211.
Davis, D.G., 2000. Extraordinary features of Lechuguilla Cave, Guadalupe Mountains. J. Cave Karst Stud. 62, 147–157.
Davis, D.G., 2012. In defense of a fluctuating-interface, particle-accretion origin of folia. Int. J. Speleol. 41 (2), 65–74.
De Vivo, B., Maiorani, A., Perna, G., Turi, B., 1987. Fluid inclusion and stable isotope studies of calcite, quartz and barite from karstic caves in the Masua mine, Southwestern Sardinia, Italy. Chem. Erde 46, 259–273.
De Waele, J., Forti, P., 2006. A new hypogean karst form: the oxidation vent. Z. Geomorphol. 147, 107–127.
De Waele, J., Forti, P., Naseddu, A., 2013. Speleogenesis of an exhumed hydrothermal sulphuric acid karst in Cambrian carbonates (Mount San Giovanni, Sardinia). Earth Surf. Process. Landf. 38 (12), 1369–1379.
De Waele, J., Audra, P., Madonia, G., Vattano, M., Plan, L., D'Angeli, I.M., Bigot, J.-Y., Nobécourt, J.-C., 2016. Sulfuric acid speleogenesis (SAS) close to the water table: examples from southern France, Austria, and Sicily. Geomorphology 253, 52–467.
De Waele, J., Gázquez, F., Forti, P., Naseddu, A., 2017. Inactive hydrothermal hypogenic karst in SW Sardinia (Italy). In: Klimchouk, A., Palmer, A., De Waele, J., Auler, A.S., Audra, P. (Eds.), Hypogene Karst Regions and Caves of the World, Cave and Karst Systems of the World. Springer, pp. 183–197.
Decker, D.D., Polyak, V.J., Asmerom, Y., 2015. Depth and timing of calcite spar and “spar cave” genesis: Implications for landscape evolution studies. In: Feinberg, J., Gao, Y., Alexander Jr.E.C. (Eds.), Caves and Karst Across Time. Geological Society of America Special Paper 516, p.
Dublyansky, Y., Spötl, C., 2009. Identifying paleo water-rock interaction during hydrothermal karstification: a stable isotope approach. In: Klimchouk, A., Ford, D.C. (Eds.), Hypogene Speleogenesis and Karst Hydrogeology of Artesian Basins, Ukrainian Institute of Speleology and Karstology, Special Paper 1, Simferopol, pp. 45–49.
Edwards, R.L., Chen, J.H., Ku, T.-L., Wasserburg, G.J., 1987. Precise timing of the last interglacial period from mass spectrometric determination of thorium-230 in corals. Science 236, 1547–1553.
Eiler, J.M., 2007. “Clumped-isotope” geochemistry—the study of naturally-occurring, multiply-substituted isotopologues. Earth Planet. Sci. Lett. 262, 309–327.
Fairchild, I.J., Smith, C.L., Baker, A., Fuller, L., Spötl, C., Mattey, D., McDermott, F., E.I.M.F, 2006. Modification and preservation of environmental signals in speleothems. Earth Sci. Rev. 75, 105–153.
Ferry, J.M., Passey, B.H., Vasconcelos, C., Eiler, J.M., 2011. Formation of dolomite at 40-80°C in the Latemar carbonate buildup, dolomites, Italy, from clumped isotope thermometry. Geology 39, 571–574.
Fornós, J.J., Gelabert, B., Ginés, A., Ginés, J., Tuccimei, P., Vesica, P., 2002. Phreatic overgrowths on speleothems: a useful tool in structural geology in littoral karstic landscapes. The example of eastern Mallorca (Balearic Islands). Geodin. Acta 15, 113–125.
Forti, P., 2010. Genesis and evolution of the caves in the Naica mine (Chihuahua, Mexico). Z. Geomorphol. 54 (2), 115–135.
Gázquez, F., Calaforra, J.M., 2013. Origin of double-tower raft cones in hypogenic caves. Earth Surf. Process. Landf. 38, 1655–1661.
Gázquez, F., Calaforra, J.M., Forti, P., Rull, F., Martínez- Frías, J., 2012a. Gypsum-carbonate speleothems from Cueva de las Espadas (Naica mine, Mexico): mineralogy and palaeohydrogeological implications. Int. J. Speleol. 41 (2), 211–220.
Gázquez, F., Calaforra, J.M., Rull, F., 2012b. Boxwork and ferromanganese coatings in hypogenic caves: an example from Sima de la Higuera Cave (Murcia, SE Spain). Geomorphology 177–178, 158–166.
Gázquez, F., Calaforra, J.M., Stoll, H., Sanna, L., Forti, P., Lauritzen, S.E., Delgado, A., Rull, F., Martínez-Frías, J.M., 2013a. Isotope and trace element evolution of the Naica aquifer (Chihuahua,Mexico) over the past 60,000 yr revealed by speleothems. Quat. Res. 80, 510–521.
Gázquez, F., Calaforra, J.M., Forti, P., De Waele, J., Sanna, L., Rull, F., Sanz, A., 2013b. Corrosion of calcite crystals by metal-rich mud in caves: study case in Crovassa Ricchi in Argento cave (SW Sardinia, Italy). Geomorphology 198, 138–146.
Gázquez, F., Calaforra, J.M., Rodriguez-Estrella, T., Ros, A., Lamusi, J.L., Sanchez, J., 2017. Evidence for regional Hypogene Speleogenesis in Murcia (SE Spain). In: Klimchouk, A., Palmer, A., De Waele, J., Auler, A.S., Audra, P. (Eds.), Hypogene Karst Regions and Caves of the World, Cave and Karst Systems of the World. Springer, pp. 183–197.
Ghosh, P., Patecki, M., Rothe, M., Brand, W.A., 2006. ^{13}C–^{18}O bonds in carbonate minerals: a new kind of palaeothermometer. Geochim. Cosmochim. Acta 70, 1439–1456.
Hellstrom, J., 2003. Rapid and accurate U/Th dating using parallel ion-counting multi-collector ICP-MS. J. Anal. Atom. Spect. 18, 1346–1351.
Hill, C.A., Forti, P., 1997. Cave Minerals of the World, 2nd edition. Nat. Speleol. Soc, Huntsville 463 p.
Klimchouk, A.B., Palmer, A., De Waele, J., Auler, A.S., Audra, P., 2017. Hypogene Karst Regions and Caves of the World, Cave and Karst Systems of the World. Springer, Cham 911 p.
Jennings, J.N., 1985. Karst Geomorphology. Basil Blackwell, Oxford 293 p.
Jones, B., 1989. Calcite rafts, Peloids, and Micrite in cave deposits from Cayman Brac, British-west-indies. Can. J. Earth Sci. 26, 654–664.
Kele, S., Breitenbach, S.F.M., Capezzuoli, E., Nele Meckler, A., Ziegler, M., Millan, I.M., Kluge, T., Deák, J., Hanselmann, K., John, C.M., Yan, H., Liu, Z., Bernasconi, S.M., 2015. Temperature dependence of oxygen- and clumped isotope fractionation in carbonates: a study of travertines and tufas in the 6–95 °C temperature range. Geochim. Cosmochim. Acta 168, 172–192.
Kim, S.-T., O'Neil, J.R., Hillaire-Marcel, C., Mucci, A., 2007. Oxygen isotope fractionation between synthetic aragonite and water: Influence temperature and Mg concentration. Geochim. Cosmochim. Acta 71, 4704–4715.
Klimchouk, A.B., 2007. Hypogene speleogenesis: hydrogeological and morphogenetic perspective. In: National Cave and Karst Research Institute Special Paper #1, Carlsbad, (106 p).
Klimchouk, A.B., 2009. Morphogenesis of hypogenic caves. Geomorphology 106, 100–117.
Klimchouk, A.B., Tymokhina, E.I., Amelichev, G.N., 2012. Speleogenetic effects of interaction between deeply derived fracture-conduit flow and intrastratal matrix flow in hypogene karst settings. Int. J. Speleol. 41 (2), 37–55.
Kluge, T., Affek, H.P., Zhang, Y., Dublyansky, Y., Spötl, C., Immenhauser, A., Richter, D.K., 2014a. Clumped isotope thermometry of cryogenic cave carbonates. Geochim. Cosmochim. Acta 126, 541–554.
Kluge, T., Affek, H.P., Dublyansky, Y., Spötl, C., 2014b. Devils hole paleotemperatures and implications for oxygen isotope equilibrium fractionation. Earth Planet. Sci. Lett. 400, 251–260.
Kovacs, S.E., Reinhardt, E.G., Chatters, J.C., Rissolo, D., Schwarz, H.P., Collins, S.V., Kim, S.-T., Blank, A.N., Erreguerena, P.L., 2017. Calcite raft geochemistry as a hydrological proxy for Holocene aquifer conditions in Hoyo Negro and Ich Balam (Sac Actun Cave System), Quintana Roo, Mexico. Quat. Sci. Rev. 175, 97–111.
LaRock, E.J., Cunningham, K.I., 1995. Helictite bush formation and aquifer cooling in wind cave, wind cave national park, South Dakota. J. Cave Karst Stud. 57 (1), 43–51.
Leél-Őssy, S., Szanyi, G., Surányi, G., 2011. Minerals and speleothems of the József-hegy cave (Budapest, Hungary). Int. J. Speleol. 40, 191–203.
Meckler, A.-N., Ziegler, M., Breitenbach, S.F.M., Millan, I., Bernasconi, S.M., 2014. Long-term performance of the Kiel carbonate device with a new correction scheme for clumped isotope measurements. Rapid Commun. Mass Spectrom. 28, 1705–1715.
Messina, M., Naseddu, A., Papinuto, S., Sanna, F., Sotgia, S., Forti, P., De Waele, J., 2005. Le esplorazioni speleologiche della miniera di San Giovanni: prime sintesi. In: De Waele, J., Naseddu, A. (Eds.), Le Grotte di Miniera: Tra economia mineraria ed economia turistica. Vol. 17. Memorie dell'Istituto Italiano di Speleologia, pp. 69–86.
Pagliara, A., De Waele, J., Forti, P., Galli, E., Rossi, A., 2010. Speleothems and speleogenesis of the hypogenic Santa Barbara cave system (South-West Sardinia, Italy). Acta Carsol. 39 (3), 551–564.
Palmer, A.N., 2011. Distinction between epigenic and hypogenic caves. Geomorphology 134, 9–22.
Palmer, M.V., Palmer, A.N., 2012. Petrographic and isotopic evidence for late-stage processes in sulfuric acid caves of the Guadalupe Mountains, New Mexico, USA. Int. J. Speleol. 41 (2), 231–250.
Piccini, L., 2000. Il carsismo di origine idrotermale del Colle di Monsummano (Pistoia–Toscana) [the hydrothermal-origin karst from the Monsummano Hills (Pistoia–Tuscany)]. Le Grotte d'Italia 1, 33–43.
Piccini, L., De Waele, J., Galli, E., Polyak, V.J., Bernasconi, S.M., Asmerom, Y., 2015. Sulphuric acid speleogenesis and landscape evolution: Montecchio cave, Albegna river valley (Southern Tuscany, Italy). Geomorphology 229, 134–143.
Picotti, V., Pazzaglia, F.J., 2008. A new active tectonic model for the construction of the

Northern Apennines mountain front near Bologna (Italy). J. Geophys. Res. 113. B005307.
Plan, L., De Waele, J., 2011. Folia in der Odelsteinhöhle, Steiermark. Erstnachweis im deutschsprachigen Raum. Die Höhle 62, 54–57.
Plan, L., Tschegg, C., De Waele, J., Spötl, C., 2012. Corrosion morphology and cave wall alteration in an Alpine sulfuric acid cave (Kraushohle, Austria). Geomorphology 169, 45–54.
Polyak, V.J., Provencio, P., 2001. By-product materials related to H_2S–H_2SO_4 influenced speleogenesis of Carlsbad, Lechuguilla, and other caves of the Guadalupe Mountains, New Mexico. J. Cave Karst Stud. 63 (1), 23–32.
Hill, C.A., Polyak, V.J., 2010. Karst hydrology of Grand Canyon, Arizona, USA. J. Hydrol. 390, 169–181.
Polyak, V.J., Duchene, H.R., Davis, D.G., Palmer, A.N., Palmer, M.V., Asmerom, Y., 2013. Incision history of Glenwood Canyon, Colorado, USA, from the uranium-series analyses of water-table speleothems. Int. J. Speleol. 42 (3), 193–202.
Rossetti, V., Zucchini, A., 1956. Baritina della Grotta di Santa Barbara. Rendiconti del Seminario della Facoltà di Scienze Università di Cagliari 26 (3–4), 240–255.
Sauro, F., De Waele, J., Onac, B.P., Galli, E., Dublyansky, Y., Baldoni, E., Sanna, L., 2014. Hypogenic speleogenesis in quartzite: the case of Corona 'e Sa Craba Cave (SW Sardinia, Italy). Geomorphology 211, 77–88.
Shen, C.-C., Wu, C.-C., Cheng, H., Edwards, R.L., Hsieh, Y.-T., Gallet, S., Chang, C.-C., Li, T.-Y., Lam, D.D., Kano, A., Hori, M., Spötl, C., 2012. High-precision and high resolution carbonate ^{230}Th dating by MC-ICP-MS with SEM protocols. Geochim. Cosmochim. Acta 99, 71–86.
Spötl, C., Vennemann, T.W., 2003. Continuous-flow isotope ratio mass spectrometric analysis of carbonate minerals. Rapid Commun. Mass Spectrom. 17, 1004–1006.
Stafford, K.W., Raymond, N., Rosales-Lagarde, L., Boston, P.J., 2008. Epigene and hypogene gypsum karst manifestations of the castile formation: Eddy County, New Mexico and Culberson County, Texas, USA. Int. J. Speleol. 37, 83–98.
Talma, A.S., Vogel, J.C., 1992. Late Quaternary paleotemperatures derived from a speleothem from Cango Caves, Cape Province, South Africa. Quat. Res. 37, 203–213.
Urey, H.C., 1948. Oxygen isotopes in nature and in the laboratory. Science 108, 489.
Vardanjani, H.K., Bahadorinia, S., Ford, D.C., 2017. An Introduction to Hypogene Karst Regions and Caves of Iran. In: Klimchouk, A.B., Palmer, A.N., De Waele, J., Auler, A.S., Audra, P. (Eds.), Hypogene Karst Regions and Caves of the World, Cave and Karst Systems of the World. Springer, pp. 479–494.
Wildberger, A., 1987. Höhlenkegel und damit verknüpfte Sinterformationen im Hölloch (Zentralschweiz) sowie daraus abgeleitete Hinweise zur Höhlenentwicklung. In: Acte 8° Congress National of the Speleological Society, Switzerland, pp. 137–142.